



**Universiteit  
Leiden**  
The Netherlands

## **Understanding and Targeting Coronaviruses: exploring advanced cell culture models and host-directed antiviral strategies**

Thaler, M.

### **Citation**

Thaler, M. (2024, July 2). *Understanding and Targeting Coronaviruses: exploring advanced cell culture models and host-directed antiviral strategies*. Retrieved from <https://hdl.handle.net/1887/3765868>

Version: Publisher's Version

License: [Licence agreement concerning inclusion of doctoral thesis in the Institutional Repository of the University of Leiden](#)

Downloaded from: <https://hdl.handle.net/1887/3765868>

**Note:** To cite this publication please use the final published version (if applicable).

# Chapter 4

## R-propranolol has broad-spectrum anti-coronavirus activity and suppresses factors involved in pathogenic angiogenesis

Melissa Thaler<sup>1</sup>, Clarisse Salgado-Benvindo<sup>1</sup>, Anouk Leijts<sup>1</sup>, Ali Tas<sup>1</sup>, Dennis K. Ninaber<sup>2</sup>, Jack L. Arbiser<sup>3,4</sup>, Eric J. Snijder<sup>1</sup>, Martijn J. van Hemert<sup>1</sup>

<sup>1</sup> Department of Medical Microbiology, Leiden University Medical Center, Leiden, The Netherlands

<sup>2</sup> Department of Pulmonology, Leiden University Medical Center, Leiden, The Netherlands

<sup>3</sup> Department of Dermatology, Emory University School of Medicine, Atlanta, GA, USA

<sup>4</sup> Division of Dermatology, Veterans Affairs Medical Center, Decatur, GA, USA

## Abstract

The SARS-CoV-2 pandemic highlighted the need for broad-spectrum antivirals to increase our preparedness. Patients often require treatment by the time that blocking virus replication is less effective. Therefore, therapy should not only aim to inhibit the virus, but also to suppress pathogenic host responses, e.g. leading to microvascular changes and pulmonary damage. Clinical studies previously linked SARS-CoV-2 infection to pathogenic intussusceptive angiogenesis in the lungs, involving upregulation of angiogenic factors like ANGPTL4. The  $\beta$ -blocker propranolol is used to suppress aberrant ANGPTL4 expression in treatment of hemangiomas. We therefore, investigated the effect of propranolol on SARS-CoV-2 infection and expression of ANGPTL4. SARS-CoV-2 upregulated ANGPTL4 in endothelial and other cells, which could be suppressed with R-propranolol. The compound also inhibited replication of SARS-CoV-2 in Vero-E6 cells and reduced viral load by up to  $\sim 2$  log in various cell lines and primary human airway epithelial cultures. R-propranolol is as effective as S-propranolol, but lacks the latter's undesired  $\beta$ -blocker activity. R-propranolol also inhibited SARS-CoV and MERS-CoV. It inhibited a post-entry step of the replication cycle, likely via host factors. The broad-spectrum antiviral effect and suppression of factors involved in pathogenic angiogenesis make R-propranolol an interesting molecule to explore further for treatment of coronavirus infections.

## Introduction

Severe acute respiratory syndrome coronavirus 2 (SARS-CoV-2) emerged in 2019 and expanded the class of highly pathogenic human coronaviruses, also including SARS-CoV and Middle East respiratory syndrome-CoV (MERS-CoV). Although the lethality of SARS-CoV-2 infection is lower compared to SARS-CoV and MERS-CoV, its transmissibility is much higher, and its fast spread led to an unprecedented pandemic and an enormous burden on health care systems worldwide. The gravity of its associated disease, COVID-19, has called for the fast development of antiviral therapies or the repurposing of existing approved drugs. Although patients are often presenting only mild or even no symptoms, elderly people or those with underlying conditions can experience severe pulmonary damage and acute respiratory distress syndrome (ARDS) that can include endothelial and vascular damage, thromboinflammation, neutrophilic and macrophage dysfunction, immunopathology, and intussusceptive angiogenesis (302). The epithelium-endothelium environment during infection and pathological changes in the lung microvascular system have been investigated in several studies (303-305). Early in the pandemic, morphological changes like

intussusceptive angiogenesis in the lungs of deceased patients were described as distinct features of COVID-19, compared to influenza virus-infected or healthy lungs (306). While formation of new blood vessels is usually a well-regulated process in for example wound healing, unregulated angiogenesis can have negative implications leading to pathogenesis (305). Intussusceptive angiogenesis is a rapid process of blood vessel neof ormation that happens due to splitting of an existing vessel into two, as opposed to sprouting angiogenesis. While the implications of vascular changes for response and repair to different lung pathologies are not well understood, it was reported that viral infections can dysregulate these processes by creating a pro-angiogenic environment of inflammation and hypoxia (307, 308). In line with these microvascular changes, transcriptional analysis identified upregulation of angiogenic factors, like *angptl4* and *VEGFA*, to a magnitude that appears unique for COVID-19 (306, 309). Angiogenic dysregulation and therapeutic interventions to control this process have been widely studied in the field of cancer research. One common type of tumor involving dysregulated blood vessel formation is infantile hemangioma. Propranolol, an approved and widely used non-selective  $\beta$ -blocker, is used to treat this condition, as this compound has also been shown to inhibit pro-angiogenic (transcription) factors (310, 311). Propranolol is a mixture of two enantiomers, R- and S-propranolol. Opposed to its S- counterpart, R-propranolol does not exert beta-blocker activity, but was shown to reduce the angiogenic factor ANGPTL4 (more efficiently) in hemangioma stem cells (310). Anti-angiogenic drugs are also used as safe treatment for idiopathic pulmonary fibrosis (312). Bevacizumab, a monoclonal antibody with anti-angiogenic property, is also evaluated in a clinical trial for its efficacy to reduce angiogenesis and vascular damage in COVID-19 patients (313). Therefore, in this study we aimed to investigate the effect of R-propranolol on the expression of angiogenesis factors that are induced by SARS-CoV-2 infection and to study its effect on virus replication. Besides an effect on ANGPTL4 expression, we - surprisingly - also uncovered a potent antiviral effect of Propranolol against a broad spectrum of highly pathogenic coronaviruses. The emergence of SARS-CoV-2 as the third highly pathogenic coronavirus within 2 decades, shows the importance of developing broad-spectrum antivirals to prepare us for future outbreaks. The repurposing of already approved and safe drugs can present a faster and more efficient way into the clinic when an outbreak calls for a swift response. Our study suggests that the approved drug R-propranolol could function as a 'double-edged sword', inhibiting both virus replication and pathogenic host responses to infection. It might therefore be an interesting drug to explore further in clinical trials.

## Results

### SARS-CoV-2 infection upregulates angiogenic factor *angptl4* in endothelial cells

To investigate whether the lung pathology-associated upregulation of angiogenic factors that was reported in COVID-19 patients, could also be observed in cell culture, we used Hulec-5a human lung endothelial cells as a relevant model for microvascular changes. We monitored expression of *angptl4*, which encodes for the Angiopoietin-like 4 protein and was reported to be upregulated in the lungs of COVID-19 patients (306). Hulec-5a cells could not be infected by SARS-CoV-2, which was also previously reported (303). These cells were also not susceptible to SARS-CoV, but could be infected with MERS-CoV, as indicated by the positive immunofluorescence staining for the viral membrane protein (M) and dsRNA (Figure 1a). Since Hulec-5a cells could not be infected with SARS-CoV-2, we used conditioned medium from SARS-CoV-2 infected Calu-3 lung epithelial cells, to mimic the epithelium-endothelium environment during infection. When Hulec-5a cells were incubated with conditioned medium we measured an increase in *angptl4* expression by RT-qPCR, in line with the reported effect of infection on the transcriptional changes in endothelial cells of patients (Figure 1b).

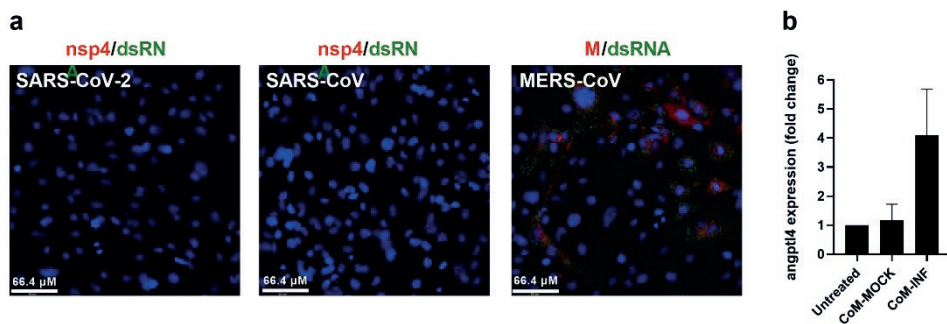


**Figure 1: Infection of Hulec-5a lung endothelial cells with various coronaviruses and expression of angiogenic factor *angptl4*.** (a) Hulec-5a cells were infected with SARS-CoV-2, SARS-CoV and MERS-CoV (Multiplicity of infection (MOI) 5) and after 48 h cells were fixed and stained with rabbit polyclonal anti-SARS-CoV nsp4 protein antibody for SARS-CoV-2 and SARS-CoV, rabbit polyclonal anti-MERS-CoV M protein antibody for MERS-CoV, mouse monoclonal anti-dsRNA antibody (J2) and with Hoechst, and visualized by immunofluorescence microscopy. Images are representative for results from 3 independent experiments. (b) Hulec-5a cells were incubated with conditioned medium from infected Calu-3 lung epithelial cells (CoM) for 24 h (diluted 1:1 with fresh medium). Intracellular RNA was isolated to quantify *angptl4* expression by RT-qPCR, using PGK1 as reference gene. n=3 independent experiments

## R-Propranolol downregulates expression of the angiogenic factor *angptl4*

Angiogenic factors like ANGPTL4 are also upregulated in infantile hemangiomas and their expression can be suppressed with the drug Propranolol, or more specifically, the stereoisomer R-propranolol. R-propranolol exerts its inhibitory effect on angiogenic factors without having beta-blocker activity (310) and therefore, we aimed to investigate the effect of R-propranolol on the expression of SARS-CoV-2 induced angiogenesis factors. Since Hulec-5a cells were not susceptible to SARS-CoV-2 (**Figure 1**), we tested if *angptl4* expression was also upregulated during infection of Vero E6 cells and whether treatment with R-propranolol would suppress it. Vero E6 cells were treated with 50  $\mu$ M of R-propranolol and were infected with SARS-CoV-2 at a MOI of 1. Analysis of total intracellular RNA isolated from infected cells at 16 hpi showed a strong increase in *angptl4* expression (**Figure 2a**). When infected cells were treated with R-propranolol, there was a significant reduction in *angptl4* expression, compared to untreated infected cells. Interestingly, when we measured intracellular viral RNA copies in those samples, we observed a 100-fold reduction in viral load in R-propranolol-treated cells compared to the infected untreated cells (**Figure 2b**). To uncouple the direct effect of R-propranolol on *angptl4* expression from its effect on virus replication, we used the chemical inducer phorbol-12-myristate-13-acetate (PMA) to increase *angptl4* expression. In Hulec-5a cells we observed that R-propranolol caused a moderate but significant downregulation of the PMA-induced increase in *angptl4* expression (**Figure 2c**). This suggested that at least part of the effect of R-propranolol on this angiogenic factor is independent from its effect on virus replication.

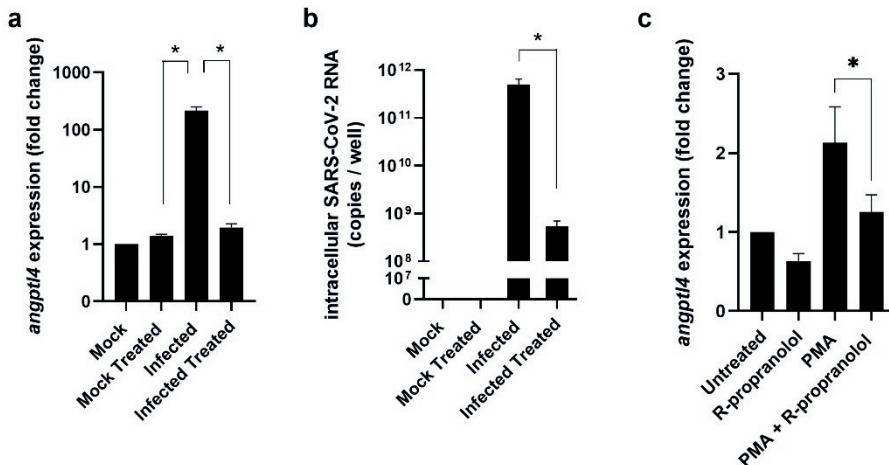


**Figure 2: Effect of R-propranolol on the upregulation of *angptl4* by infection or PMA treatment.** Vero E6 cells were infected with SARS-CoV-2 (MOI 1) in the absence or presence of 50  $\mu$ M R-propranolol. (a) the fold increase

in *angptl4* RNA levels compared to untreated uninfected cells (Mock) and (b) intracellular viral RNA copies were quantified by RT-qPCR at 16 hpi. n=2 independent experiments (c) Hulec-5a cells were treated with 0.1  $\mu$ M PMA and 6 h later 50  $\mu$ M R-Propranolol was added. 12 h later the increase in *angptl4* expression was quantified by RT-qPCR. n=2 independent experiments. For normalization the levels of reference gene PGK1 were measured by RT-qPCR for all experiments. Data are mean  $\pm$  SEM. Statistical analysis was conducted using ratio paired t-test and significant differences are indicated by \*P<0.05.

## R- and S-propranolol inhibit SARS-CoV-2 replication in cell culture

Quantification of intracellular viral RNA in the experiments to study *angptl4* expression suggested that R-propranolol inhibited virus replication. We therefore, assessed the effect of the compound in more detail in various antiviral assays. The marketed drug Propranolol contains a mixture of the stereoisomers S- and R-propranolol. We therefore assessed the effect of both S- and R-propranolol in cytopathic effect (CPE) reduction assays with SARS-CoV-2. Vero E6 cells were infected at a low MOI in the presence of compound, and after 72 h cell viability was measured by MTS assay. R-propranolol protected cells from infection with an IC<sub>50</sub> of 12  $\mu$ M (**Figure 3a**). S-propranolol inhibited SARS-CoV-2 replication with an IC<sub>50</sub> of 15  $\mu$ M (**Figure 3b**). We observed no cytotoxicity in uninfected cells that were treated in parallel with the same increasing concentrations of compounds. Since R-propranolol was slightly more effective than S-propranolol, and is devoid of the undesired beta-blocker activity, we decided to perform all further experiments with R-propranolol.

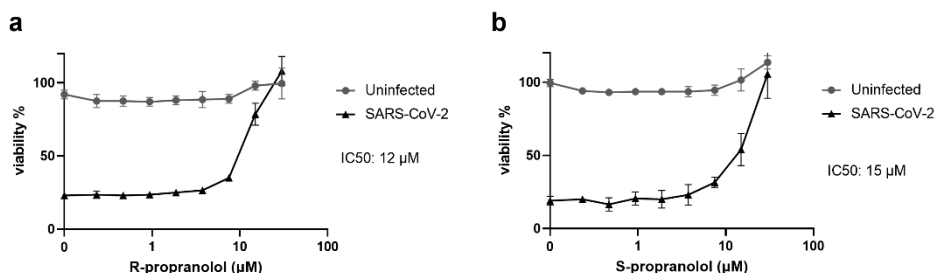


**Figure 3: Effect of R-propranolol and S-propranolol on SARS-CoV-2-induced cytopathic effect in Vero E6 cells.** CPE reduction assays were done on Vero E6 cells infected with SARS-CoV-2 (MOI of 0.015). Cells were pre-treated with and infected in the presence of (a) R-Propranolol, or (b) S-Propranolol. At 72 hpi cell viability was determined by MTS assay. n=2 independent experiments. Cell viability of uninfected compound-treated cells was measured in parallel to assess cytotoxicity of the compound. Mean  $\pm$  SEM are shown. The 50% inhibitory concentration (IC<sub>50</sub>) was determined by non-linear regression with GraphPad Prism 6.

### R-propranolol inhibits SARS-CoV-2 replication in various cell lines and air–liquid interface cultured primary human airway epithelial cells

To validate the antiviral effect of R-propranolol that was observed in CPE reduction assays (Fig. 3), we performed viral load reduction assays. Vero E6 cells were pre-treated with compound, infected at a MOI of 1 and at 16 hpi the viral load was determined by quantifying the number of extracellular viral RNA copies by RT-qPCR. In this single replication cycle experiment R-propranolol caused a significant and up to 100-fold reduction in extracellular viral RNA copies (**Figure 4a**), with a 90% effective concentration (EC90) of 20  $\mu\text{M}$ . To assess whether the compound was also able to prevent spread of infection in human lung cells, we infected the human lung epithelial cell line H1299-hACE2 at an MOI of 0.001, treated it with compound and measured viral load after multiple rounds of replication at 48 hpi (**Figure 4b**). In this infection model we also observed a 100-fold reduction in viral load and an EC90 of 26  $\mu\text{M}$ . Measurement of cell viability by MTS assay showed that the compound caused no cytotoxicity at the concentrations used in both cell lines.

To analyze the efficacy of R-propranolol in a more advanced infection model, we used primary bronchial epithelial cells that were cultured at the air-liquid interface (ALI-PBEC). This infection model efficiently recapitulates the pseudostratified epithelium of the lung and its infection by coronaviruses (Thaler et al., manuscript under revision). ALI-PBEC were infected with SARS-CoV-2 (MOI of  $\sim 0.1$ ) and treated with 100  $\mu\text{M}$  of R-propranolol on the apical side of the cells during the 2 h inoculation with virus. Infected control cells were treated with PBS instead of compound (“untreated” control). The compound was also added to the medium on the basal side of the cells and remained present until 48 hpi, when samples were harvested. We observed a significant reduction in viral load for R-propranolol treated cells compared to untreated controls (**Figure 4c**). Measurement of cell death (by LDH release) in untreated and treated ALI-PBEC indicated that R-propranolol caused no significant cytotoxicity under these conditions (**Figure 4d**).

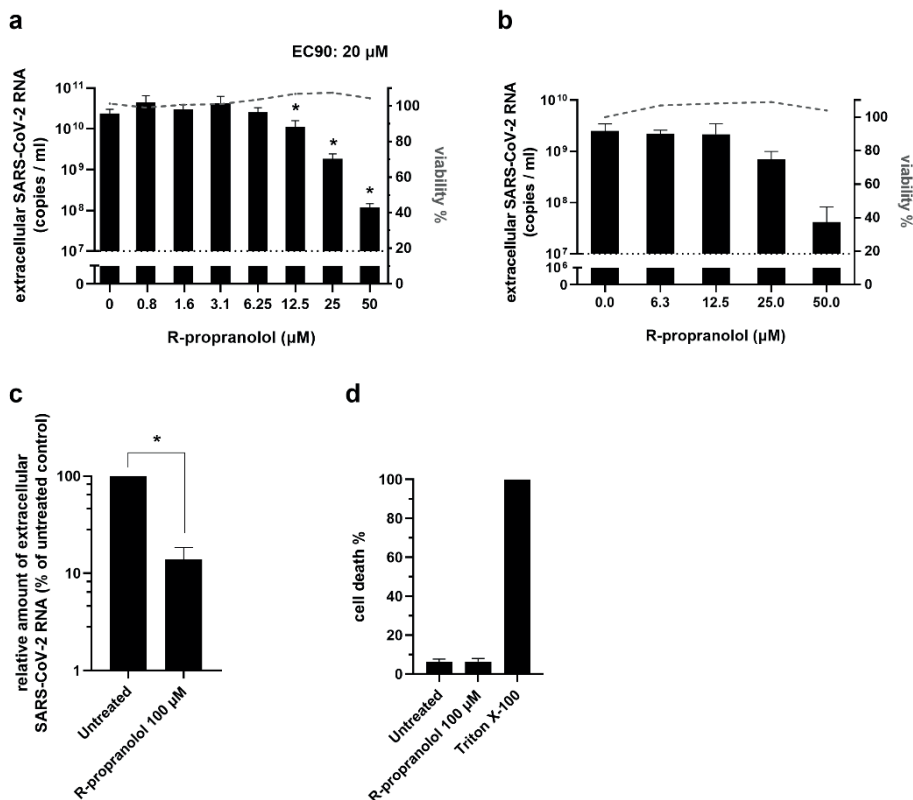


**Figure 4: Effect of R-propranolol on replication of SARS-CoV-2 in Vero E6 and H1299-hACE2 cells and primary human bronchial epithelial cell cultures grown at the air-liquid interface (ALI-PBEC).** (a) Viral load reduction assay on Vero E6 cells. Cells were infected with a MOI of 1 and at 16 hpi extracellular viral RNA copy numbers were determined by RT-qPCR. n=3 independent experiments. (b) H1299-hACE2 cells were infected at MOI 0.001 and the viral load in the medium at 48 hpi was determined by RT-qPCR. n=2 independent experiments. In parallel, cell viability of uninfected Vero E6 and H1299-hACE2 cells treated with R-propranolol was measured by MTS assay and data were normalized to untreated uninfected cells (% viability). (c) ALI-PBEC were treated with 100  $\mu$ M R-propranolol and inoculated with SARS-coV-2 for 2 h (MOI  $\sim$ 0.1) in the presence of compound. After removal of the inoculum, the viral load in the apical wash was determined at 48 hpi. R-propranolol remained present in the basal medium until 48 hpi. n=3 independent experiments. Mean  $\pm$  SEM are shown for all experiments. (d) In ALI-PBEC cytotoxicity was monitored by quantifying the release of LDH and data were normalized to ALI-PBEC treated with Triton X-100 (100 % cell death). n=2 independent experiments. Statistical analysis was conducted using two-way ANOVA with a Tukey/Bonferroni post-hoc test or in (c) with a t-test. Significant differences are indicated by \*P<0.05.

## R-propranolol inhibits SARS-CoV-2 at a post-entry step of the replication cycle

To elucidate the mode of action of R-propranolol, we first evaluated whether the compound affects the infectivity of viral particles, i.e. has virucidal activity. We therefore incubated SARS-CoV-2 with 50 or 150  $\mu\text{M}$  of the compound for 1 h at 37  $^{\circ}\text{C}$ , before assessing the (remaining) number of infectious particles by plaque assay. Control treatment with 70% ethanol led to complete inactivation of the virus, but R-propranolol had no effect on the infectious titer compared to the untreated virus stock (**Figure 5a**).

To elucidate which step of the viral life cycle is affected by R-propranolol we performed a time-of-addition assay (**Figure 5b**). The strongest reduction in viral load was observed when cells were pretreated and the compound remained present during infection until the time of harvesting. Although less effective, treatment initiated at 2 hpi still reduced viral load, suggesting that the compound does not target attachment/entry of the virus. This was further supported by the observation that pretreatment alone (2 or 4 hours prior to infection) or presence of the compound in the inoculum only during infection (0-1 hpi) did not reduce the viral load. Together these results suggested that R-propranolol inhibited a post entry step of the replication cycle, possibly via its effect on a host factor(s).

To obtain more insight into the mode of action we compared the specific infectivity of treated and untreated samples (**Figure 5c**). Infectious progeny and extracellular genome copies were reduced to the same extent by R-propranolol treatment, suggesting the compound does not affect infectivity of viral genomes (e.g. does not compromise genome integrity) and does not affect the infectivity of released particles. It leads to an overall reduction in the release of infectious particles.

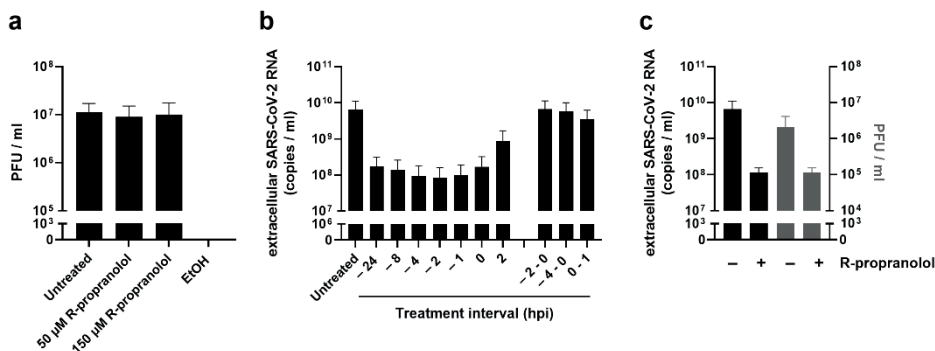


**Figure 5: R-propranolol inhibits replication of SARS-CoV-2 at a post-entry step.** (a) Effect of the compound on infectivity of SARS-CoV-2. Virus was incubated with either 50 or 150  $\mu\text{M}$  R-propranolol, 70% ethanol, or medium (untreated control) for 1 h at 37  $^{\circ}\text{C}$ . Remaining infectivity was measured by plaque assay. n=3 independent experiments (b) Time of addition assay with Vero E6 cells infected at MOI 1 and R-propranolol treatments during

the intervals indicated at the X-axis or initiated at the time points indicated after which compound remained present until 16 hpi. Supernatant was harvested at 16 h post infection and extracellular viral RNA was measured by RT-qPCR n=2 independent experiments (c) Supernatant of infected Vero E6 cells at 16 hpi, untreated or treated with 50  $\mu$ M R-propranolol was analyzed by RT-qPCR and plaque assay. Mean  $\pm$  SEM are shown.

## R-propranolol has broad-spectrum antiviral activity against different coronaviruses

We assessed the activity of R-propranolol against various SARS-CoV-2 variants in viral load reduction assays and found that the delta and omicron variants were inhibited by R-propranolol too (Fig 6A). We then evaluated its effect on different highly pathogenic coronaviruses. The compound also inhibited SARS-CoV replication in Vero E6 cells (Figure 6b) and MERS-CoV replication in HuH-7 cells (Figure 6c), suggesting it has a broad spectrum activity against coronaviruses.

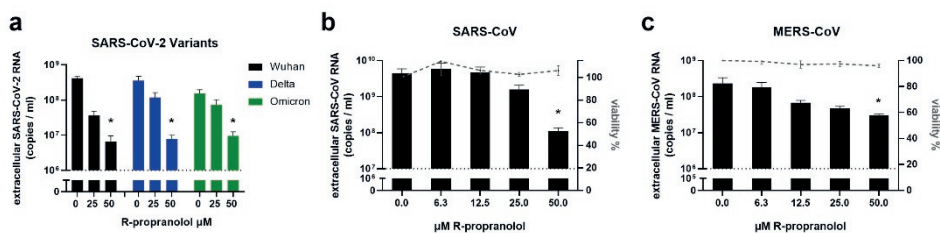


**Figure 6: Effect of R-propranolol on replication of SARS-CoV-2 variants, SARS-CoV and MERS-CoV.** (a) Viral load reduction assay on Vero E6 cells with SARS-CoV-2 variants. The viral load at 16 hpi was determined by RT-qPCR and cell viability was monitored in parallel. N=2 independent experiments. (b) Viral load reduction assay with SARS-CoV in Vero E6 cells infected at MOI 1. Viral load at 16 hpi was determined by RT-qPCR and cell viability was monitored in parallel. N=3 independent experiments. (c) HuH-7 cells were infected with MERS-CoV (MOI 1) and 16 hpi viral load was determined by RT-qPCR. N=3 independent experiments. Mean  $\pm$  SEM are shown. Statistical analysis was conducted using two-way ANOVA with a Tukey/Bonferroni post-hoc test. Significant differences are indicated by \*P<0.05. Cell viability of uninfected cells treated with compound was determined in parallel using MTS assay and data were normalized to untreated uninfected cells (100 % viability).

## Discussion

Despite the unprecedented successes of vaccine development in response to the SARS-CoV-2 pandemic, the demand for safe and effective antiviral drugs remains. Not only to treat COVID-19 patients but also to better prepare us for future coronavirus outbreaks, as such drugs could be used prophylactically, post-exposure or in outbreak settings when vaccines to new threats are not yet available. Since COVID-19 patients often present with serious

symptoms rather late there is not only a need for drugs that directly inhibit virus replication, but also for therapeutics that target the (pathogenic) host responses to infection. Hallmarks of severe SARS-CoV-2 infection are pulmonary inflammation, tissue damage and microvascular changes in the lung. Pathogenic angiogenesis and upregulation of pro-angiogenic factors like ANGPTL4 have been observed in patients with severe SARS-CoV-2 or influenza virus infections (306). Recently, increased ANGPTL4 plasma levels were associated with higher proportions of ARDS and increased hospital mortality (309). In mice deficient for ANGPTL4, influenza virus infection led to less pulmonary damage (314), suggesting that suppression of the SARS-CoV-2-induced upregulation of ANGPTL4 might be a strategy to counteract the pathogenic angiogenesis that can be caused by SARS-CoV-2 infection. In this study we explored the potential therapeutic effect of R-propranolol on COVID-19 pathophysiology, and uncovered its broad-spectrum antiviral effect against coronaviruses. The approved drug propranolol is a non-selective  $\beta$ -adrenergic blocker that is mainly used to treat cardiovascular problems. However, it also has a beta-blocker-independent effect on angiogenesis and is therefore used to treat infantile hemangiomas (310). Propranolol consists of the stereoisomers R-propranolol and S-propranolol, of which R-propranolol is devoid of beta blocker activity. R-propranolol was shown to reduce the pro-angiogenic factor ANGPTL4 in a murine hemangioma model, without having beta-blocker activity and thus circumventing potential side effects that could be caused by the beta-blocker activity of S-propranolol. We therefore, also focused our studies on R-propranolol and confirmed the inhibitory effect of this compound on chemically induced *angptl4* expression in lung endothelial cells. Lung endothelial cells were not susceptible to SARS-CoV-2, but treatment of endothelial cells with conditioned medium from SARS-CoV-2-infected epithelial cells caused an increase in *angptl4* expression. This underlines the impact of the epithelium-endothelium crosstalk during infection and the consequences for the microvascular system. *Angptl4* expression was also upregulated in SARS-CoV-2-infected Vero E6 cells and this effect could be suppressed by treatment with R-propranolol. Future studies will need to address the effect of infection and R-propranolol in more advanced (organoid and *in vivo*) models to assess whether the compound could have therapeutic effect on exacerbated angiogenesis.

Besides the effect on expression of virus-induced angiogenic factors, we also observed that R-propranolol inhibits virus replication. Our study for the first time uncovered a direct antiviral effect of R-propranolol that supports previous clinical observations on the apparent (indirect) beneficial effect of propranolol on the outcome of viral infections (315). R-propranolol treatment of infected Vero E6 cells protected them from cytopathic effects with an EC<sub>50</sub> of 12  $\mu$ M, slightly more effective than S-propranolol, which had an EC<sub>50</sub> of 15  $\mu$ M. Treatment of infected cells also led to a significant reduction in extracellular viral RNA

copies with an EC<sub>90</sub> of 20  $\mu$ M and the compound also reduced the viral load by 2 logs in a lung cell line infection model. Finally, we employed primary bronchial epithelial cells cultured at the air-liquid interface as most relevant infection system, as it efficiently reconstitutes the pseudostratified lung epithelium and its infection. In this model R-propranolol also reduced the viral load in the apical wash of the culture without causing any noticeable cytotoxicity.

Furthermore we could show that R-propranolol has broad-spectrum activity against different SARS-CoV-2 variants, including delta and omicron, and it also inhibited other highly pathogenic coronaviruses, i.e. SARS-CoV and MERS-CoV. The compound had no virucidal effect and time of addition assays suggested that it inhibits a post-entry step of the replication cycle. Its broad-spectrum activity and its enhanced activity upon pretreatment suggest that R-propranolol likely inhibits viral replication via one or more host factors. These likely play no role in the attachment or entry of the viral particle, since there was no reduction in viral load when the compound was present only during infection (in the inoculum). R-propranolol reduced the amount of infectious progeny that was released from cells, but did not appear to affect the specific infectivity, suggesting it does not affect infectivity of particles or integrity of the genome (e.g. does not lead to mutations or defects in capping). While we were preparing this manuscript, a preprint was published on the effect of R-propranolol on SARS-CoV-2 and MHV replication, including the observation of an inhibitory effect on MHV replication in a mouse model (316). The findings of this study were in line with our data and the compound was suggested to affect replication complex formation through an effect on phospholipid synthesis, which corroborates our results (in time of addition assays). Previous studies on propranolol-induced changes in gene expression in endothelial cells also included genes involved in lipid and sterol metabolism and ubiquitination (317). Propranolol also has an effect on various other host factors and signalling pathways, including inhibition of the RAS/RAF/ERK and AKT pathways (318, 319). Inhibition of factors involved in these signalling pathways was also shown to affect SARS-CoV-2 replication (320). Therefore, to unravel the compound's mode of action, more in-depth research is required to elucidate which host factor(s) or pathway(s) contribute to the R-propranolol-mediated inhibition of coronavirus replication.

It is also important to keep in mind that most of the studies on the activity of propranolol or its separate stereoisomers have been done in the context of cancer research. Therefore, these findings might not be directly translatable to non-cancer models and need to be investigated in proper infection models. Widespread use of Propranolol renders it a safe and interesting drug to be investigated further, and the use of the enantiomer R-propranolol which has no beta-blocker activity lowers the risk of possible negative side-effects. Its inhibition of virus replication and suppression of detrimental host responses to

infection make R-propranolol an interesting compound for further evaluation in clinical studies.

## Materials and Methods

### Compounds and Cell Culture

R-(+)-Propranolol hydrochloride, S-(+)-Propranolol hydrochloride and phorbol-12-myristate-13-acetate (PMA) were purchased from MedChemExpress and dissolved in DMSO.

Vero E6 cells and HuH-7 cells were cultured as previously described (321). Human lung cell line H1299-hACE2 will be described elsewhere (Salgado-Benvindo et al, manuscript in preparation). These cells were cultured in Dulbecco's modified Eagle's medium with 4.5 g/l glucose with L-glutamin (DMEM; Lonza, Switzerland), supplemented with 10% fetal calf serum (FCS)(CapriCorn Scientific, USA), 100 U/ml of Penicillin/Streptomycin (P/S) (Sigma-Aldrich) and 1200 µg/ml G418 for selection (InvivoGen). Calu-3 cells (ATCC, HTB-55TM) were cultured in Eagle's minimum essential medium (EMEM, Lonza), supplemented with 9% FCS, 1% non-essential amino acids (NEAA, Sigma-Aldrich), 2 mM L-glutamine (Sigma-Aldrich), 1 mM sodium pyruvate (Sigma-Aldrich) and 100 U/ml of P/S.

Infections of Vero E6 cells, HuH-7 cells, H1299-hACE2 cells and Calu-3 cells were performed in Eagle's minimal essential medium with 25 mM HEPES (EMEM; Lonza) supplemented with 2% FCS, 2mM L-glutamine (Sigma-Aldrich), and 100 U/ml of P/S (referred to as infection medium).

Primary human bronchial epithelial cells (PBEC) were isolated and cultured as previously described (322). Hulec-5a cells were purchased from ATCC and cultured and infected in EGM<sup>TM</sup>-2 MV Microvascular Endothelial Cell Growth Medium-2 BulletKit<sup>TM</sup>. Hulec-5a cells were used between passage 2 and 6. Infections of Hulec-5a cells were done in culture medium, treatment with PMA was done in infection medium.

All cell cultures were maintained at 37 °C in an atmosphere of 5% CO<sub>2</sub>.

### Virus stocks

All experiments with infectious SARS-CoV, SARS-CoV-2 or MERS-CoV were performed at the LUMC biosafety level 3 facilities. For Vero E6 infections the clinical isolate SARS-CoV-2/Leiden-0002 (isolated at LUMC during the first wave of the Corona pandemic in March 2020 (GenBank: MT510999.1) was used. For H1299-hACE2 and ALI-PBEC infections SARS-CoV-2/Leiden-0008 (isolated at LUMC during the first wave of the Corona pandemic in

March 2020 (GenBank: MT705206.1) was used, as it was not adapted to Vero E6 cells with regard to the spike S1/S2 cleavage site (confirmed by NGS sequencing). SARS-CoV-2 variant BA.1 (Omicron) was obtained from RIVM (strain hCoV-19/Netherlands/NH-RIVM-72291/2021, lineage B.1.1.529), and variant B.1.617 (Delta) was obtained from the University of Leuven. SARS-CoV-2/Leiden-0002 (Passage 3), SARS-CoV-2/Leiden-0008 (Passage 2), SARS-CoV isolate Frankfurt 1 (298) (Passage 4), Omicron (Passage 3) and Delta (Passage 4) variant were grown in Vero E6 cells. MERS-CoV (N3/Jordan) (GenBank: KJ614529.1) (Passage 3) was grown on HuH-7 cells. Virus titers were determined by plaque assay on Vero E6 cells, and for MERS-CoV and on HuH-7 cells, as described before (255).

### Endothelial cell infection

Hulec-5a cells were seeded on glass coverslips at a density of  $8 \times 10^4$  cells/well in a 12-well plate and infected with SARS-CoV, SARS-CoV-2 or MERS-CoV at a MOI of 5 in 500  $\mu$ l medium per well. 48 h later cells were fixed and processed as previously described (122). Cells were stained with rabbit polyclonal anti-SARS-CoV nsp4 protein antibody (FGQ4) for SARS-CoV-2 and SARS-CoV, rabbit polyclonal anti-MERS-CoV M protein antibody (R9004) for MERS-CoV and with mouse monoclonal anti-dsRNA antibody (J2). Secondary antibodies used were a Cy3-conjugated donkey anti-rabbit IgG antibody (Jackson ImmunoResearch Laboratories) and an Alexa488-conjugated goat anti-mouse IgG antibody (Invitrogen).

### Endothelial cell (drug) treatments

Hulec-5a cells were incubated with conditioned medium from Calu-3 lung epithelial cells (CoM) for 24 h (diluted 1:2 with fresh medium). Intracellular RNA was isolated to quantify *angptl4* expression by RT-qPCR. For CoM, Calu-3 cells were seeded at a density of  $2.4 \times 10^5$  cell/well in 6-well plates and infected with SARS-CoV-2 (Leiden-008) at a MOI of 1 for 2 h at 37°C on a rocking platform. The inoculum was removed, cells were washed with PBS three times and 500  $\mu$ l infection medium was added. At 48 hpi medium was harvested and stored at -80°C.

For treatment with PMA, Hulec-5a cells were seeded at a density of  $7 \times 10^3$  cells/well in a 96-well plate. After 24 h medium was changed to infection medium. After 16 h, cells were treated with 100 nM PMA for 6 h. Then R-propranolol was added and cells were incubated for 12 h. Control wells were treated with only PMA, R-propranolol or medium (untreated). Then intracellular RNA was harvested and *angptl4* expression was quantified by RT-qPCR.

### **Cytopathic effect (CPE) reduction assay**

CPE reduction assay was performed as previously described (234). Briefly, Vero E6 cells were seeded in 96-well plates at a density of  $5 \times 10^3$  cells per well. The next day, cells were incubated with 2-fold serial dilutions of R- or S-propranolol starting at 50  $\mu\text{M}$  and subsequently infected. 3 days post infection the CellTiter 96 aqueous nonradioactive cell proliferation kit (Promega) was used to measure cell viability of infected (protection) and non-infected cells (assessment of cytotoxicity).

### **Viral load reduction assays**

Viral load reduction assays were performed as previously described (234). Briefly Vero E6 cells were infected with SARS-CoV-2, SARS-CoV-2 variants or SARS-CoV, and HuH-7 cells were infected with MERS-CoV, at a MOI of 1. Pretreatment with R-propranolol was done for 4 h. Alternatively (Figure 2) Vero E6 cells were seeded at a density of  $7 \times 10^4$  cells/well in 24-well plates. Cells were pretreated 2 h with 50  $\mu\text{M}$  R-propranolol and infected with SARS-CoV-2 at a MOI of 1. At 16 hpi total intracellular RNA was harvested and viral RNA copies (intracellular & extracellular) and *angptl4* expression were quantified by multiplex RT-qPCR, using PGK1 as reference gene.

### **Time of Addition Assay**

Vero E6 cells were seeded in 24-well cell culture plates at a density of  $2 \times 10^4$  cells/well. Cells were incubated with 50  $\mu\text{M}$  of R-Propranolol in 500  $\mu\text{l}$  infection medium at the indicated timepoints. 48h after seeding, cells were infected with  $8 \times 10^4$  PFU of virus per well (MOI 1) in 200  $\mu\text{l}$  of medium. Supernatant was harvested at 16 hpi and extracellular viral RNA copies were measured by RT-qPCR (255).

### **Virucidal effect assay**

Vero E6 cells were seeded in 6-well cell culture plates at a density of  $3.5 \times 10^5$  cells/well. The next day, virus ( $3 \times 10^5$  PFU) was incubated, in a total of 60  $\mu\text{l}$ , at 37 °C with 50 or 150  $\mu\text{M}$  compound, only medium or ethanol (66% end concentration). After incubation for 1 h, 50  $\mu\text{l}$  samples were serially diluted to lower the compound and ethanol concentration to a level that did not inhibit the subsequent plaque assay to determine the remaining infectious virus titer (255).

## **Viral infection of ALI-PBEC**

The apical side of the cells was washed with 200  $\mu$ l warm PBS for 10 min at 37 °C to remove excess mucus and cellular debris and basal medium was refreshed prior to infection. Cells were infected with 100,000 PFU of SARS-CoV-2 in 200  $\mu$ l PBS (with or without compound) per insert for 2 h at 37 °C on a rocking platform (estimated multiplicity of infection [MOI] of 0.1). For noninfected (mock) controls the same procedure was performed with only PBS. After removal of the inoculum, the apical side of the cells was washed three times with PBS. At 48 hpi, 200  $\mu$ l of PBS was added to the apical side of the cells and after incubation for 10 min at 37 °C, supernatant was harvested to quantify the viral load by RT-qPCR.

## **RNA isolation and RT-qPCR**

RNA was isolated either using Tripure isolation reagent (Sigma-Aldrich) or by magnetic bead isolation. Briefly, 20  $\mu$ l of SpeedBeads™ carboxylate-modified magnetic particles (Merck) and 135  $\mu$ l of isopropanol were added to 100  $\mu$ l of supernatant in a 96-well plate. The plate was placed on a magnetic rack for 15 min, then supernatant was removed, and beads were washed one time with 150  $\mu$ l of isopropanol and then two times with 200  $\mu$ l of 70% ethanol. The beads were air-dried and, after removal of the plate from the magnetic rack, resuspended in 50  $\mu$ l RNase free water for 3 min. The plate was placed back on the magnetic rack for 10 min to collect the eluate containing total RNA. Equine arteritis virus (EAV) RNA in AVL lysis buffer (Qiagen) was spiked into the reagent as an internal control for extracellular RNA samples. The cellular reference gene PGK1 served as a control for intracellular RNA. Primers and probes for EAV and PGK1 and the normalization procedure were described before (255). Viral RNA was quantified by RT-qPCR using TaqMan Fast Virus 1-step master mix (Thermo Fisher Scientific) and as previously described (234). Primers and probes for SARS-CoV-2 and SARS-CoV, as well as a standard curve, were used as described previously (234, 256), and for MERS-CoV with final primer concentrations of 450 nM each and probe concentrations of 200 nM. Angptl4 was quantified using the ANGPTL4 TaqMan® Gene Expression Assay FAM-MGB (ThermoFisher, Catalog No. 4331182, ID Hs01101123\_g1).

## **Author Contributions**

Conceptualization, M.T., M.vH., J.A.; methodology, M.T., M.vH.; investigation, M.T. C.S.B, A.L, A.T; resources, D.N, J.A; writing—original draft preparation, M.T, M.vH.; writing—review and editing, M.T, J.A., E.S., M.vH.; visualization, M.T; supervision, E.S., M.vH; project

administration, M.vH.; funding acquisition, M.vH.. All authors have read and agreed to the published version of the manuscript.

## **Funding**

Clarisse Salgado-Benvindo was supported by the Coordination for the Improvement of Higher Education Personnel (CAPES) (Process nr. 88881.171440/2018-01), Ministry of Education, Brazil.

**Institutional Review Board Statement:** Not applicable

## **Informed Consent Statement**

Informed consent was obtained from all subjects involved in the study. Primary bronchial epithelial cells were isolated from macroscopically normal lung tissue obtained from patients undergoing resection surgery for lung cancer at the Leiden University Medical Center, the Netherlands. Patients from which this lung tissue was derived were enrolled in the biobank via a no-objection system for coded anonymous further use of such tissue ([www.coreon.org](http://www.coreon.org)). However, since 29-11-2020, patients are enrolled in the biobank using active informed consent in accordance with local regulations from the LUMC biobank with approval by the institutional medical ethical committee (B20.042/Ab/ab and B20.042/Kb/kb).

## **Data Availability Statement**

Data is contained within the article

## **Acknowledgments**

We thank Dr. Anne van der Does<sup>2</sup> for advice and help with handling the Hulec-5a cells.

## **Conflicts of Interest**

The authors declare no conflict of interest. The funders had no role in the design of the study; in the collection, analyses, or interpretation of data; in the writing of the manuscript; or in the decision to publish the results.

**Disclaimer/Publisher's Note:** The statements, opinions and data contained in all publications are solely those of the individual author(s) and contributor(s) and not of MDPI and/or the editor(s). MDPI and/or the editor(s) disclaim responsibility for any injury to people or property resulting from any ideas, methods, instructions or products referred to in the content.

## References

1. Bösmüller H, Matter M, Fend F, Tzankov A. The pulmonary pathology of COVID-19. *Virchows Archiv : an international journal of pathology*. 2021 Jan;478(1):137-50.
2. Wang P, Luo R, Zhang M, Wang Y, Song T, Tao T, et al. A cross-talk between epithelium and endothelium mediates human alveolar–capillary injury during SARS-CoV-2 infection. *Cell Death & Disease*. 2020 2020/12/08;11(12):1042.
3. Bordoni V, Mariotti D, Matusali G, Colavita F, Cimini E, Ippolito G, et al. SARS-CoV-2 Infection of Airway Epithelium Triggers Pulmonary Endothelial Cell Activation and Senescence Associated with Type I IFN Production. *Cells*. 2022 Sep 17;11(18).
4. Solimando AG, Marziliano D, Ribatti D. SARS-CoV-2 and Endothelial Cells: Vascular Changes, Intussusceptive Microvascular Growth and Novel Therapeutic Windows. 2022; *Biomedicines* 10(9):2242.
5. Ackermann M, Verleden SE, Kuehnel M, Haverich A, Welte T, Laenger F, et al. Pulmonary Vascular Endothelialitis, Thrombosis, and Angiogenesis in Covid-19. 2020; *N Engl J. Med* 383(2):120-28.
6. Caposio P, Orloff SL, Streblov DN. The role of cytomegalovirus in angiogenesis. *Virus Res*. 2011 May;157(2):204-11.
7. Hassan M, Selimovic D, El-Khattouti A, Soell M, Ghozlan H, Haikel Y, et al. Hepatitis C virus-mediated angiogenesis: molecular mechanisms and therapeutic strategies. *World journal of gastroenterology*. 2014 Nov 14;20(42):15467-75.
8. Bhatraju PK, Morrell ED, Stanaway IB, Sathe NA, Srivastava A, Postelnicu R, et al. Angiopoietin-Like 4 is a Novel Marker of COVID-19 Severity. 2023. *Critical care explorations*. Jan;5(1):e0827.
9. Zhang L, Mai HM, Zheng J, Zheng JW, Wang YA, Qin ZP, et al. Propranolol inhibits angiogenesis via down-regulating the expression of vascular endothelial growth factor in hemangioma derived stem cell. *International journal of clinical and experimental pathology*. 2014;7(1):48-55.
10. Sasaki M, North PE, Elsej J, Bublej J, Rao S, Jung Y, et al. Propranolol exhibits activity against hemangiomas independent of beta blockade. *NPJ Precis Oncol*. 2019;3:27-27.
11. Varone F, Sgalla G, Iovene B, Bruni T, Richeldi L. Nintedanib for the treatment of idiopathic pulmonary fibrosis. *Expert Opinion on Pharmacotherapy*. 2018 2018/01/22;19(2):167-75.
12. Pang J, Xu F, Aondio G, Li Y, Fumagalli A, Lu M, et al. Efficacy and tolerability of bevacizumab in patients with severe Covid-19. *Nat Commun*. 2021 Feb 5;12(1):814.
13. Li L, Chong Han C, Ng Say Y, Kwok Ka W, Teo Z, Tan Eddie Han P, et al. Angiopoietin-like 4 Increases Pulmonary Tissue Leakiness and Damage during Influenza Pneumonia. *Cell Reports*. 2015 2015/02/10;10(5):654-63.
14. Peuschel KE. Some clinical evidence of the hypothesis of an indirect antiviral effect of propranolol through immunoactivation. *Med Hypotheses*. 2011 2011/05/01;76(5):689-91.
15. Fang H, Wang Y, Liu L, Cheng K, Li P, Tan Y, et al. A Host-Harbored Metabolic Susceptibility of Coronavirus Enables Broad-Spectrum Targeting. Preprint *bioRxiv*. 2022:2022.12.07.519404.

16. Stiles J, Amaya C, Pham R, Rowntree RK, Lacaze M, Mulne A, et al. Propranolol treatment of infantile hemangioma endothelial cells: A molecular analysis. *Exp Ther Med*. 2012 2012/10/01;4(4):594-604.
17. Zhou C, Chen X, Zeng W, Peng C, Huang G, Li X, et al. Propranolol induced G0/G1/S phase arrest and apoptosis in melanoma cells via AKT/MAPK pathway. *Oncotarget*. 2016 Oct 18;7(42):68314-27.
18. Hu Q, Liao P, Li W, Hu J, Chen C, Zhang Y, et al. Clinical Use of Propranolol Reduces Biomarkers of Proliferation in Gastric Cancer. *Frontiers in oncology*. 2021;11:628613.
19. Klann K, Bojkova D, Tascher G, Ciesek S, Münch C, Cinatl J. Growth factor receptor signaling inhibition prevents SARS-CoV-2 replication. *Molecular Cell*. 2020 2020/08/11/.
20. Salgado-Benvindo C, Leijts AA, Thaler M, Tas A, Arbiser JL, Snijder EJ, et al. Honokiol inhibits SARS-CoV-2 replication in cell culture. 2023 *Microbiol Spectr*.
21. Wang Y, Thaler M, Ninaber DK, van der Does AM, Ogando NS, Beckert H, et al. Impact of human airway epithelial cellular composition on SARS-CoV-2 infection biology. 2023 *J. Innate Immun*
22. Drosten C, Günther S, Preiser W, Van Der Werf S, Brodt H-R, Becker S, et al. Identification of a novel coronavirus in patients with severe acute respiratory syndrome. *New England journal of medicine*. 2003;348(20):1967-76.
23. Kovacicova K, Morren BM, Tas A, Albulescu IC, van Rijswijk R, Jarhad DB, et al. 6'-β-Fluoro-Homoaristeromycin and 6'-Fluoro-Homoneplanocin A Are Potent Inhibitors of Chikungunya Virus Replication through Their Direct Effect on Viral Nonstructural Protein 1. *Antimicrob Agents Chemother*. 2020 Mar 24;64(4).
24. Ogando NS, Dalebout TJ, Zevenhoven-Dobbe JC, Limpens R, van der Meer Y, Caly L, et al. SARS-coronavirus-2 replication in Vero E6 cells: replication kinetics, rapid adaptation and cytopathology. *The Journal of general virology*. 2020 Sep;101(9):925-40.
25. Salgado-Benvindo C, Thaler M, Tas A, Ogando NS, Bredenbeek PJ, Ninaber DK, et al. Suramin Inhibits SARS-CoV-2 Infection in Cell Culture by Interfering with Early Steps of the Replication Cycle. *Antimicrob Agents Chemother*. 2020 Jul 22;64(8).
26. Corman VM, Landt O, Kaiser M, Molenkamp R, Meijer A, Chu DK, et al. Detection of 2019 novel coronavirus (2019-nCoV) by real-time RT-PCR. *Euro Surveill*. 2020 Jan;25(3).

